ELSEVIER

Thin Solid Films 313–314 (1998) 614–619

thin solid films

Real-time optical characterization of GaP heterostructures by p-polarized reflectance

N. Dietz[a,*], K. Ito[b]

[a] *Department of Physics, North Carolina State University, Raleigh, NC 27695, USA*
[b] *Center for Research in Scientific Computation, North Carolina State University, Raleigh, NC 27695, USA*

Abstract

The stringent tolerances in the engineering of advanced optoelectronic integrated circuits with respect to control thickness and composition of ultra-thin layers require the development of monitoring and control techniques that follow the deposition process with sub-monolayer resolution. These demands led to the development of surface-sensitive real-time optical sensors that are able to move the control point close to the point where the growth occurs, which in a chemical beam epitaxy process is the surface reaction layer, built up of physisorbed and chemisorbed precursor fragments between the ambient and film interface. In this contribution, we explore the application of p-polarized reflectance spectroscopy (PRS) in the context of real-time monitoring and control of pulsed chemical beam epitaxy (PCBE) during low temperature growth of epitaxial GaP heterostructures on Si(001) substrates by PCBE. The effect of periodic alterations in composition and thickness of a surface reaction layer (SRL) is monitored by PRS as a periodic modulated reflectance amplitude, denoted as fine structure. Using a 'reduced order kinetic model' we demonstrate the linkage of the PRS response towards surface reaction chemistry, film growth rate, and film properties. Mathematical control algorithms are introduced that link the PR signals to the growth process control parameters. © 1998 Elsevier Science S.A.

Keywords: P-polarized reflectance spectroscopy; Pulsed chemical beam epitaxy; Reduced order kinetic model

1. Introduction

Research concerning the integration of polar compound semiconductors on non-polar Si substrates is motivated by several decades of technological applications and is becoming even more important with regard to the advanced state of silicon technology. However, the progress in understanding and controlling thin film growth has been very slow, considering how little is known about chemical reaction pathways and reaction kinetics parameters during the decomposition process of the metal-organic (MO) precursors. To gain a better understanding of the deposition process and the surface chemistry involved, non-intrusive real-time optical process techniques have been developed during the last decade, which focus on the monitoring of either bulk-film properties [1–4] or surface processes by reflection high energy electron diffraction (RHEED) or reflectance difference spectroscopy (RDS) [5]. For real-time closed-loop deposition control, a product-driven virtual substrate approach was recently introduced [6]. For monitoring both the bulk and surface, we have recently added p-polarized reflectance spectroscopy (PRS) and demonstrated its capability during pulsed chemical beam epitaxy (PCBE) of III-V heteroepitaxial growth. The demonstrated high sensitivity of PRS towards surface reaction processes in the context of real-time monitoring of PCBE has opened new possibilities for characterization and control of thin film deposition processes [7–13]. So far, the PR response during heteroepitaxial $GaP/Ga_xIn_{1-x}P$ growth on Si under

* Corresponding author. Tel.: +1 919 5152867; fax: +1 919 5193419; e-mail: dietz@mte.nscu.edu

PII S0040-6090(97)00896-1

PCBE conditions has been modeled under the simplified assumption of a surface reaction layer (SRL) periodically modulated in thickness. The modulation in composition and, with it, the modulation in the dielectric function of the SRL have been neglected. Control of a growth process using the optical signature from the SRL that feeds the underlying growth requires detailed instantaneous simulation and prediction of the surface chemistry and its link to the optical properties of the outermost layer in a multilayer stack. In this contribution, we introduce a reduced order kinetic model to describe the growth process with a mathematically reduced number of surface reaction equations using heteroepitaxial GaP growth as an example.

2. Surface chemistry

In the case of GaP heteroepitaxy on Si employing triethylgallium [TEG, $Ga(C_2H_5)_3$] and tertiarybutylphosphine [TBP, $(C_4H_9)PH_2$] as source vapors, efficient fragmentation and sufficient retention of fragments on the surface occurs within a limited process window in the temperature range 533 K $\leq T \leq$ 683 K for Si(100) [14]. The kinetics of TEG pyrolysis for the growth of GaP on Si(100) utilizing triethylgallium and tertiary-butylphosphine as source vapors has been discussed in detail elsewhere [13,15]. Its progression can be summarized in three consecutive steps:

$$Ga(C_2H_5)_3 \rightarrow Ga(C_2H_2)_2^{\bullet} + C_2H_5^{\bullet}, \quad (1)$$

$$Ga(C_2H_5)_2 \rightarrow |GaC_2H_5 + C_2H_5^{\bullet}, \quad (2)$$

$$|GaC_2H_5 \rightarrow |Ga^{\bullet} + C_2H_5^{\bullet}, \quad (3)$$

where the vertical dashes and superscript dots denote lone electron pairs and single valence electrons, respectively. Also, the thermal decomposition of TBP has been studied in detail [16,17] and proceeds through a series of consecutive reactions, that can be summarized by [13]

$$(C_4H_9)PH_2 \rightarrow |PH_2^{\bullet} + C_4H_9^{\bullet}, \quad (4)$$

$$C_4H_9^{\bullet} + (C_4H_9)PH_2 \rightarrow (C_4H_9)\overline{P}H^{\bullet} + C_4H_{10} \quad (5)$$

and

$$|C_4H_9|\overline{P}H^{\bullet} \rightarrow |\overline{P}H + C_4H_9^{\bullet}. \quad (6)$$

The vertical dashes and superscript dots denote lone electron pairs and single valence electrons, respectively. For GaP growth on Si(100), we have shown that the decomposition of TBP is fast and elimination of ethyl radicals from the TEG fragments represents the rate limiting step [18]. Depending on the delay between the TEG and TBP source vapor pulses, carry-over of TEG fragments from one precursor pulse cycle to the next may occur, which establishes in steady-state a surface reaction layer (SRL), consisting of a mixture of reactants and products of the chemical reactions that drive the epitaxial growth process. In a realistic model, the SRL represents a multicomponent mixed phase with a variety of radical reactions added to the above reactions (1)–(6) [18]. The thickness and composition of the SRL depends on the relative heights and widths of the employed TEG and TBP source vapor pulses and their repetition rate. We note that some of the intermediate fragments of the source vapor molecules in the SRL that feed III-V CBE, such as H-$\overline{V}^{\bullet}$-H, $|\overline{V}$-H, R-III$^{\bullet}$-R, |III-R carry a permanent dipole moment. Thus dipole-dipole interactions are likely to contribute to the stabilization of the SRL. In view of intermolecular interactions, deviations of the SRL from ideal behavior can be expected. The objective of this paper is to relate the measured PRS signal to the activities of the reactants and products in the SRL, and lay the foundation for the use of PRS in investigations of the kinetics of epitaxial growth and real-time modeling for closed loop process control. Based on the above reaction chemistry, we model the linkage between the measured PRS signal and the surface kinetics on the basis of a reduced order kinetic model and a four-media stack: ambient/SRL/epilayer/substrate, which represents the simplest possible description of the optical response under the conditions of PCBE processes.

3. Reduced order kinetic model

For the interpretation of the time-dependence of the four media stack reflectance, $R_4(t)$, in terms of the chemical kinetics in the SRL that drives epitaxial growth, the dielectric function of the SRL, ε_1, must be linked to its composition. Such a linkage can be established via the Sellmeier equation [13]:

$$\varepsilon_1(\omega) = 1 - \frac{4\pi q^2 N_A}{m} \Sigma_l c_l \sum_{\Psi_k \rightarrow \Psi_j} \left[\frac{f_{kj}}{\omega^2 - \omega_{kj}^2 + i\omega\Gamma_{kj}} \right] = 1 - \frac{4\pi q^2 N_A}{m} \Sigma_l x_l F_l(\omega) \quad (7)$$

that describes the dielectric function of a pure substance in terms of the electronic transitions from filled states Ψ_k to empty states Ψ_j allowed by symmetry for the molecules of this particular medium [19]. The dielectric function of the SRL is obtained by summing over the contributions of all its constituents, identified by the label l. In Eq. (7), ω denotes the frequency at

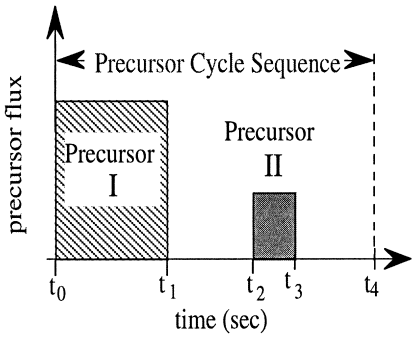

Fig. 1. Schematic representation of a precursor cycle sequence used for the growth of a binary compound semiconductor grown via two organo-metallic precursors. For GaP growth, the first precursor is TBP and the second precursor is TEG.

which ε_1 is evaluated, $-q$ and m are the electronic charge and mass. f_{kj} is the oscillator strength of the electronic transition $\Psi_k \rightarrow \Psi_j$ expressed in terms of the component of the polarization vector ξ of the exciting electromagnetic wave along the matrix element of the electric dipole operator $\mu_{kj} = -q\langle\Psi_k|\mathbf{r}|\Psi_j\rangle$. The reduced order kinetic model for the binary compound semiconductor GaP, summarizes all reactions Eqs. (1)–(6) in one dominant bimolecular reaction for the TBP pyrolysis (first precursor, PC1) and two dominant bimolecular reactions for the TEG decomposition (second precursor, PC2). Both precursors are supplied sequentially separated by pauses as shown schematically in Fig. 1. The experimental set-up and growth conditions have been described in previous publications [7,20].

With the above mentioned assumptions, the differential rate equations for the molar concentrations n_1 of SRL constituents in the GaP system can be written as

$$\frac{d}{dt}n_1(t) = n_{\mathrm{PC1}} - \tilde{a}_1 n_1(t) - \tilde{a}_4 n_3(t) n_1(t), \tag{8}$$

$$\frac{d}{dt}n_2(t) = n_{\mathrm{PC2}} - \tilde{a}_2 n_2(t), \tag{9}$$

$$\frac{d}{dt}n_3(t) = \tilde{a}_2 n_2(t) - \tilde{a}_3 n_3(t) - \tilde{a}_4 n_3(t) n_1(t) \tag{10}$$

with a final incorporation reaction

$$\frac{d}{dt}n_4(t) = \tilde{a}_4 n_3(t) n_1(t). \tag{11}$$

Eq. (8) describes the reduced order TBP pyrolysis, where n_{PC1} denotes a periodic supply function expressed in terms of the molar concentration of TBP reaching the surface; $\tilde{a}_1$ is a generalized reaction parameter for the decomposition of TBP into active surface phosphorous. Eq. (9) and Eq. (10) describe the reduced order decomposition reaction process of TEG with a periodically supplied molar concentration, n_{PC2}, of TEG and two generalized reaction parameters $\tilde{a}_2$ and $\tilde{a}_3$. The formation of GaP and its incorporation in the underlying film is summarized in the reaction Eq. (11). At this point, the SRL is treated as a homogeneous ideal solution and the surface area, A, is assumed to be constant for simplicity. Also note that the surface structure, number of reaction sides and inhomogeneous reactions are not explicitly addressed at this point and are integrated into the reaction parameter $\tilde{a}_4$.

From the system Eqs. (8)–(11) we can extract the film growth rate g_{fl} as

$$g_{fl} = \frac{1}{A}\frac{\partial}{\partial t} n_4 \tilde{V}_{\mathrm{GaP}}. \tag{12}$$

The temporal thickness evolution of the SRL is given by

$$d_1(t) = \frac{1}{A}\left[n_1\bar{V}_1 + n_2\bar{V}_2 + n_3\bar{V}_3\right]. \tag{13}$$

where $\bar{V}_l$ are the molar volumes of the constituents in the SRL. The effective dielectric function ε_1 of the SRL can be parameterized and expressed as the sum over all molar concentrations n_1 contributing to the SRL:

$$\varepsilon_1(\omega) = \varepsilon_\infty + \alpha\left[\frac{n_1(t)}{\Sigma_k n_k(t)}F_1(\omega) + \frac{n_2(t)}{\Sigma_k n_k(t)}F_2(\omega) + \frac{n_3(t)}{\Sigma_k n_k(t)}F_3(\omega)\right] \quad (k = 1,2,3) \tag{14}$$

The link to the PR signal is described in the following section.

4. Control method

The reduced order kinetic model described in Sec. 3 provides a model for the composition and thickness of the SRL, in terms of the effective dielectric function $\varepsilon_1(\omega,t)$ and $d_1(t)$, respectively. It also gives the instantaneous growth rate $g_{fl}(t)$ of the GaP film. These are incorporated in Fresnel's equation that determines the reflectance amplitude, rr, of the p-polarized light as follows. Consider the four-layer media composed of ambient/SRL/film/substrate. We model the reflection/refraction of the surface reaction layer by an effective medium with the homogeneous dielectric function $\varepsilon_1(t)$ and the thickness $d_1(t)$. Let us denote the four media by the indices $n = 0,1,2,3$ labeled from the ambient to the substrate. The reflection coefficient $r_{n-1,n}$ from the $(n-1)$-st media to n-th media is given by

$$r_{n-1,n} = \frac{\varepsilon_n\sqrt{\varepsilon_{n-1} - \varepsilon_0\sin^2\varphi} - \varepsilon_{n-1}\sqrt{\varepsilon_n - \varepsilon_0\sin^2\varphi}}{\varepsilon_n\sqrt{\varepsilon_{n-1} - \varepsilon_0\sin^2\varphi} + \varepsilon_{n-1}\sqrt{\varepsilon_n - \varepsilon_0\sin^2\varphi}} \tag{15}$$

where ε_n is the complex dielectric function of the n-th media. The factor Φ_n for the n-th media is given by

$$\Phi_n = \frac{2\pi d_n}{\lambda}\sqrt{\varepsilon_n - \varepsilon_0\sin^2\varphi}\,, \tag{16}$$

where d_n is the thickness of the n-th media. The reflectance amplitude rr_4 of p-polarized light is then given by

$$rr_4 = \frac{r_{01} + r_{12}e^{-2j\Phi_1} + r_{23}e^{-2j(\Phi_1+\Phi_2)} + r_{01}r_{12}r_{23}e^{-2j\Phi_2}}{1 + r_{01}r_{12}e^{-2j\Phi_1} + r_{01}r_{23}e^{-2j(\Phi_1+\Phi_2)} + r_{12}r_{23}e^{-2j\Phi_2}}, \tag{17}$$

or, equivalently by

$$rr_4 = \frac{r_{01} + \hat{r}e^{-2i\Phi_1}}{1 + r_{01}\hat{r}e^{-2i\Phi_1}} \quad \text{with} \quad \hat{r} = \frac{r_{12} + r_{23}e^{-2i\Phi_2}}{1 + r_{12}r_{23}e^{-2i\Phi_2}}$$

Here, r_{01}, r_{12} and Φ_1 are functions in $\varepsilon_1(t)$ and $d_1(t)$. Since r_{23} is a given constant (dielectric functions for film and substrate are assumed to be fixed), we can define the function $s(t) = r_{23}e^{-2i\Phi_2(t)}$ as

$$\frac{\mathrm{d}s}{\mathrm{d}t} = \frac{-4\pi i}{\lambda}\sqrt{\varepsilon_3 - \varepsilon_0\sin^2\varphi} * g_{fl}s(t). \tag{18}$$

The PR signals at the two different angles of incidence φ_i, $I = 1,2$ are given by the real-time measurements

$$R_i(t) = |rr_4|^2 = H_i(\varepsilon_1(t), d_1(t), s(t)). \tag{19}$$

Now, for example we can formulate the problem of controlling the growth rate of GaP film as follows. One can determine

$$\min\int_0^T |g_{fl}(t) - g_d(t)|^2\mathrm{d}t \tag{20}$$

over the flow rate $f_{\mathrm{TEG}}(t)$ that establishes the molar supply concentrations n_{PC2} of TEG in Eq. (9), subject to the model dynamics described in Eqs. (8)–(10). In Eq. (20), g_d is the desired growth rate function. Suppose all reaction rate parameters $\tilde{a}_i$ and the initial conditions of $n_i(t)$, $i = 1,2,3$ in our model are known. Then we have the so-called open loop control problem in Eq. (20), and we can determine the optimal control function for $f_{\mathrm{TEG}}(t)$ by the standard control algorithm [21]. Or, the optimal control law can be given in the state feedback as

$$f_{\mathrm{TEG}}(t) = K(t, \hat{n}(t))\cdot\hat{n}(t). \tag{21}$$

The state feedback control is more robust than the open-loop control, but in order to implement the feedback control we need to observe the full state $\hat{n}(t)$.

In the case of real-time and run-to-run control problems we are not able to determine all necessary rate constants and the state variables $n_i(t)$, $I = 1,2,3$. Moreover, the reaction rate parameters a_i may be time-dependent due to temperature modulations and/or inhomogeneities in composition/thickness of the surface reaction layer. Thus, we employ the control method based on the active feedback law (21) with real-time state and parameter estimation. Specifically, the control signal $f_{\mathrm{TEG}}(t)$ is given by

$$f_{\mathrm{TEG}}(t) = K(t, \hat{n}(t), \hat{p}(t)) \tag{22}$$

where K is the state feedback law and $\hat{n}(t)$ and $\hat{p}(t)$ are estimates of the state function and the reaction rate parameter based on the PR signals. We can construct the feedback law, for example by the dynamically programming method [21] and/or by the LQR method applied to the linearization of the model Eq. (20) at the reference point. The real-time estimate of the state and the rate constants based on the PRS signals can be constructed by applying filtering algorithms based on variants of the Kalman-filter ([21], Ito, unpublished results). This approach provides a real-time control method that can be robust with respect to the temperature fluctuations and variations in the growth conditions. Also, the monitoring of the growth process can be achieved in terms of on-line estimates of the state variables.

5. Results

Fig. 2 shows the evolution of the PR signals during growth of GaP on Si(001) at 350°C, recorded for two angles of incidence, $\varphi = 68° \pm 0.1°$ and $\varphi = 74° \pm 0.1°$, at $\lambda = 690 \pm 5$ nm and at $\lambda = 632.8$ nm, respectively. A precursor cycle sequence time of 3 s has been used with a continuous hydrogen flow during the entire cycle time. The fine structure observed in the PR signal (see inset in Fig. 2) is strongly correlated to the time sequence of the supply of precursors employed during the steady-state growth of GaP. Each peak in the fine structure corresponds to a complete precursor cycle with the start of the oscillation always coinciding with the leading edge of the first TBP pulse of the sequence. As can be seen in Fig. 2, the amplitude in the fine structure undergoes periodic changes dur-

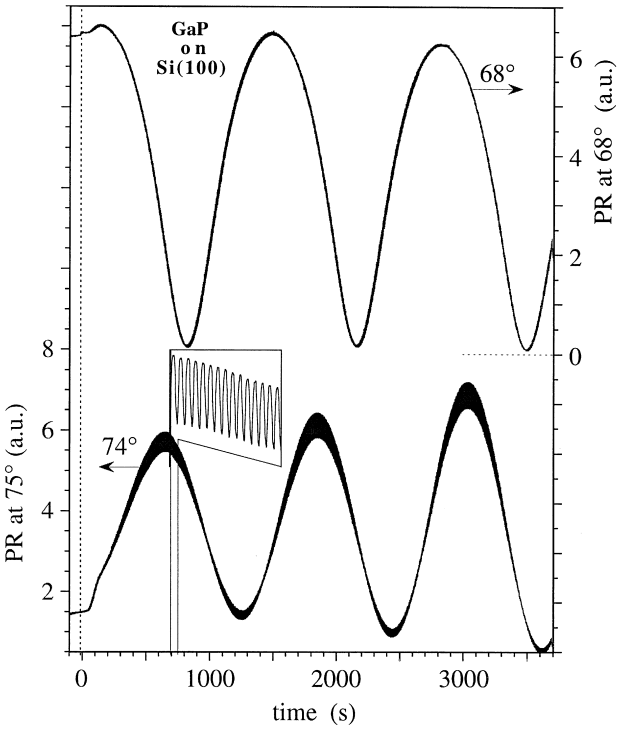

Fig. 2. Heteroepitaxial GaP growth on Si under PCBE conditions at 350°C monitored at two incidence angles, $\varphi = 68°$ and $\varphi = 74°$. The inset shows an enlargement of the PR fine structure as a response to the thickness- and composition-modulated SRL.

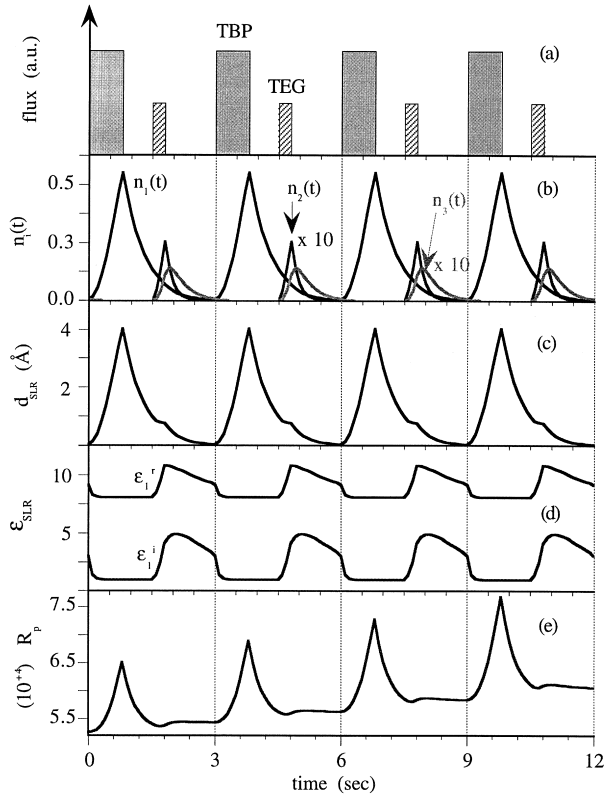

Fig. 3. Modeling of PR response during GaP growth on Si under PCBE conditions at 350°C: (a) precursor cycle sequence; (b) molar concentrations $n_i(t)$ of constituents in the SRL; (c–d) thickness $d_1(t)$ and dielectric function $\varepsilon_1(t)$ modulation; and (e) four media stack reflectance calculated for $\varphi = 74.1°$, $\lambda = 632.8$ nm and a growth rate of 0.78 Å/s.

ing the deposition time. This amplitude modulation in the fine structure can be analyzed to extract the average complex dielectric function of the SRL as well as its average thickness [12]. For GaP growth with a 3-s pulse cycle time, an average dielectric function of $\varepsilon_1 = (9.5, 2.5)$ with an average thickness of 5 Å for the SRL has been calculated with a growth rate of 0.78 Å/s [12].

Using these values, we can generate the initial starting conditions for the unknown generalized reaction rate parameters $\tilde{a}_i$ and the initial conditions of $n_i(t)$, in Eqs. (8)–(11), which are subject to parameter estimation. Fig. 3 shows the temporal evolution of $n_i(t)$, $d_1(t)$, $\varepsilon_1(t)$ and the four-media stack reflectance for a pulse cycle sequence of 3 s, where the surface is sequentially exposed to a TBP pulse from 0.0 to 0.8 s and a TEG pulse from 1.5 to 1.8 s. The molar concentrations $n_i(t)$ in Fig. 3b are the solution of the coupled differential system Eqs. (8)–(10). The thickness of the SRL and its dielectric function are computed using Eq. (13) and Eq. (14). The reflectance R_P in Fig. 3e is given by Eq. (16). These oscillations in R_P are superimposed on interference fringes, resulting from back reflection at the substrate-layer interface as shown in Fig. 4. The temporal evolution of the PR signals in Fig. 4 are simulated for two angles of incidence $\varphi = 74.1°$, and $\varphi = 68°$, with wavelengths of $\lambda = 632.8$ nm and $\lambda = 690$ nm, respectively. The fine structure shown in Fig. 3 is not resolved in Fig. 4. A comparison with the experimental data in Fig. 2 shows an excellent agreement of the overall fine structure evolution. Deviations encountered during the initial growth period are due to a changed surface chemistry during the nucleation and overgrowth process, which has not been accounted for in this model. The number of parameters involved in this simulation totals to 11, with four unknown reaction kinetics parameters to describe the decomposition and loss process, four parameters for the molar volumes and three parameters that describe the optical oscillator strength for each constituent in the SRL. Even so, some of these parameters, such as the molar volumes and optical oscillator strengths can be estimated from literature data, a larger set of experimental data is required in order to go to the next step from qualitative to quantitative analysis of surface reaction kinetics.

6. Conclusion

We introduced a reduced order kinetic model using generalized reaction rate parameters to describe the

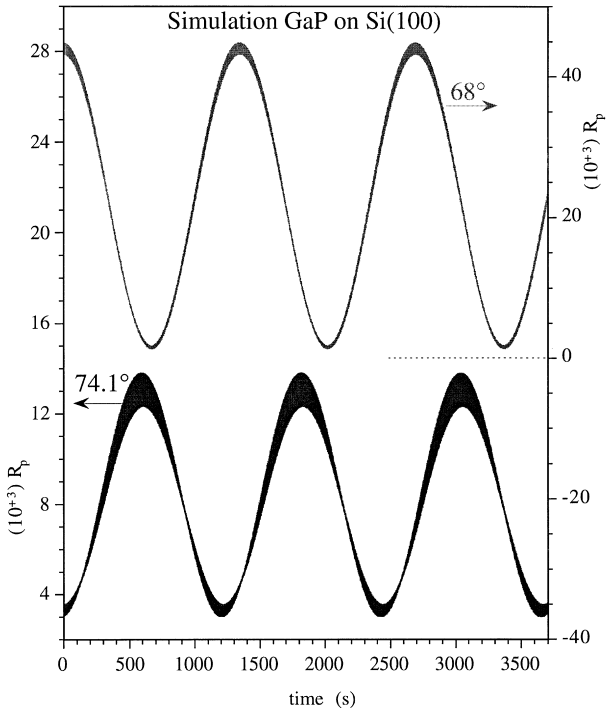

Fig. 4. Modeling of PR response at two angles of incidence, $\varphi = 74.1°$ ($\lambda = 632.8$ nm) and $\varphi = 68°$ ($\lambda = 690$ nm), simulating GaP growth on Si under PCBE conditions at 350°C.

thickness and composition evolution of the SRL. The molar concentrations n_i in the SRL are directly linked to the growth rate of the underlying film. An on-line parameter estimate of the state functions and the reaction rate parameters $\tilde{a}_i$ using the PRS signals can be used to analyze the PRS fine structure and to provide the control signal. The reduced order kinetic model provides the link between the TEG flow rate and GaP growth rate as well as the analysis of surface chemistry processes. The successful application of this approach will not only provide the closest possible feedback control-loop, but also will give a more detailed understanding of the surface reaction chemistry under steady-state thin film growth.

Acknowledgements

This work has been supported by the DOD-MURI Grant F49620-95-1-0447.

References

[1] W.G. Breiland, K.P. Killeen, Proc. Mater. Res. Soc. 406 (1995) 99.
[2] W.G. Breiland, K.P. Killeen, J. Appl. Phys. 78 (1995) 6726.
[3] K.P. Killeen, W.G. Breiland, J. Electron. Mater. 23 (1994) 179.
[4] S.D. Murthy, I.B. Bhat, B. Johs, S. Pittal, P. He, J. Electron. Mater. 24 (1995) 445.
[5] D.E. Aspnes, J.P. Harbison, A.A. Studna, L.T. Florez, Appl. Phys. Lett. 52 (1988) 957.
[6] D.E. Aspnes, IEEE J. Select. Top. Quantum Electron. 1 (1995) 1054.
[7] N. Dietz, A. Miller, K.J. Bachmann, JVST A 13 (1995) 153.
[8] K.J. Bachmann, N. Dietz, A.E. Miller, D. Venables, J.T. Kelliher, JVST A 13 (1995) 704.
[9] N. Dietz, K.J. Bachmann, Vacuum 47 (1996) 133.
[10] K.J. Bachmann, U. Rossow, N. Sukidi, H. Castleberry, N. Dietz, JVST B 14 (1996) 3019.
[11] N. Dietz, U. Rossow, D.E. Aspnes, K.J. Bachmann, Appl. Surface Sci. 102 (1996) 47.
[12] N. Dietz, N. Sukidi, C. Harris, K.J. Bachmann, JVST A 15 (1997) 807.
[13] K.J. Bachmann, N. Sukidi, N. Dietz, C. Hoepfner, S. LeSure, H.T. Tran, S. Beeler, K. Ito, H.T. Banks, J. Crystal. Growth (1997) (in press).
[14] J.T. Kelliher, N. Dietz, K.J. Bachmann, Proc. SOTAPOCS 18, Honolulu, Hawaii, The Electrochemical Society, Pennington, NJ, 1994, p. 17.
[15] A.J. Murrell, A.T.S. Wee, D.H. Fairbrother, N.K. Singh, J.S. Foord, G.J. Davies, D.A. Andrews, J. Cryst. Growth 105 (1990) 199.
[16] S.H. Li, C.A. Larsen, N.I. Buchan, G.B. Stringfellow, W.P. Kosar, D.W. Brown, J. Appl. Phys. 65 (1989) 5161.
[17] G.H. Fan, R.D. Hoare, M.E. Pemble, I.M. Povey, A.G. Taylor, J.O. Williams, J. Cryst. Growth 124 (1992) 49.
[18] K.J. Bachmann, U. Rossow, N. Dietz, Mater. Sci. Eng. B 37 (1995) 472.
[19] G. Burns, Solid State Physics, Academic Press, Orlando, 1985, 461 p.
[20] N. Dietz, K.J. Bachmann, MRS Bull. 20 (1995) 49.
[21] W.H. Fleming, R.W. Rishel, Deterministic and Stochastic Optimal Control, Springer Verlag, New York, 1975.